Four-Electron-Donor Hemilabile η^3-PPh_3 Ligand that Binds through a C=C Bond Rather than an Agostic C−H Interaction, and Displacement of the C=C by Methyl Iodide or Water

Tan-Yun Cheng,[†] David J. Szalda,[†,‡] Jonathan C. Hanson,[†] James T. Muckerman,[†] and R. Morris Bullock*[,†,§]

Chemistry Department, Brookhaven National Laboratory, Upton, New York 11973-5000, and Chemical Sciences Division, Pacific Northwest National Laboratory, P.O. Box 999, K2-57, Richland, Washington 99352

Received May 5, 2008

Hydride transfer from $Cp(CO)_2(PPh_3)MoH$ to $Ph_3C^+BAr'_4{}^-$ [Ar′ = 3,5-bis(trifluoromethyl)phenyl] produces $[Cp(CO)_2(\eta^3\text{-}PPh_3)Mo]^+[BAr'_4]^-$. Spectroscopic and crystallographic data indicate that one C=C of a Ph ring is weakly bound to the Mo, so that the PPh_3 ligand is a four-electron-donor ligand. Computations (DFT/B3LYP and MP2 on $[Cp(CO)_2(\eta^3\text{-}PPh_3)Mo]^+$ and $[Cp(CO)_2(\eta^3\text{-}PH_2Ph)Mo]^+$, and DFT/B3LYP on $[Cp(CO)_2(\eta^3\text{-}PH^tBuPh)Mo]^+$ and $[Cp(CO)_2(\eta^3\text{-}PH_2Ph)Nb]$) provide further information on the bonding and on the preference for bonding of the metal to the C=C bond rather than an agostic C−H interaction found in many related complexes. The hemilabile C=C bond is readily displaced by CH_3I or H_2O, and crystal structures are reported for $[Cp(CO)_2(PPh_3)Mo(ICH_3)]^+$ and $[Cp(CO)_2(PPh_3)Mo(OH_2)]^+$. The equilibrium constant for $[Cp(CO)_2(\eta^3\text{-}PPh_3)Mo]^+ + ICH_3$ to give $[Cp(CO)_2(PPh_3)Mo(ICH_3)]^+$ is $K_{eq} = 5.2 \times 10^2\ M^{-1}$ in CD_2Cl_2 at 22 °C.

Introduction

Organometallic complexes with a 16-electron configuration have a remarkable range of stability. Some electronically unsaturated 16-electron complexes are indefinitely stable, particularly square-planar four-coordinate complexes of Rh(I), Ir(I), Pt(II), and Pd(II). Examples include familiar complexes such as Wilkinson's catalyst, $RhCl(PPh_3)_3$, Vaska's complex, $IrCl(CO)(PPh_3)_2$, and Pt and Pd complexes of the general formula L_2MX_2 (M = Pt, Pd, L = phosphine, X = halide).

In other cases, coordinatively unsaturated metal complexes very rapidly bind another ligand to achieve an 18-electron count. An example comes from time-resolved infrared studies by Bergman, Moore, and co-workers, who found that flash photolysis of $Cp^*Rh(CO)_2$ ($Cp^* = \eta^5\text{-}C_5Me_5$) in mixtures of Kr and cyclohexane did not lead to the observation of the unsaturated 16-electron complex Cp*Rh(CO), but rather produced Cp*Rh(CO)(Kr) and Cp*Rh(CO)(cyclohexane) prior to the formation of $Cp^*Rh(CO)(H)(C_6H_{11})$.[1] This reaction documents the very strong affinity of some metal complexes for ligands, even those as weakly bound as noble gases or alkanes.

Many complexes relevant to homogeneous catalysis lie between these two extremes of reactivity. Since dissociation of a ligand to create a vacant coordination site at the metal is a required step in the mechanism of many homogeneously catalyzed reactions, complexes that weakly and reversibly bind additional ligands are of much interest. Hemilabile ligands[2] have two different types of ligand sites, one of which is readily but reversibly displaced. Weakly bound ligands can temporarily occupy and protect a vacant coordination site, so structural and reactivity studies on metal complexes with weakly bound ligands can be useful in understanding the role of such ligands in catalysis.

Triphenylphosphine has a prominent role in the development of organometallic chemistry and homogeneous catalysis. In the vast majority of examples, PPh_3 serves as a traditional two-electron donor ligand through the lone pair on the phosphorus atom. There was evidence as early as 1965 that it could function as an overall four-electron donor, through formation of a three-center, two-electron bond between one of the C−H bonds of a Ph ring and the metal.[3] Such agostic[4,5] interactions became well-recognized in later years, and additional examples of this type of bonding were found for PPh_3 and related phosphines.[6–9] We found that the PPh_3 ligand in $[Cp(CO)_2(PPh_3)Mo]^+[BAr'_4]^-$ [Ar′ = 3,5-bis(trifluoromethyl)phenyl] is a chelating, bidentate four-electron donor, *not* involving an agostic C−H bond, but rather an interaction in which one C=C of one phenyl ring binds

* Corresponding author. E-mail: morris.bullock@pnl.gov.
† Brookhaven National Laboratory.
‡ Reasearch collaborator at Brookhaven National Laboratory. Permanent address: Department of Natural Sciences, Baruch College, New York, NY.
§ Pacific Northwest National Laboratory.

(1) (a) Schultz, R. H.; Bengali, A. A.; Tauber, M. J.; Weiller, B. H.; Wasserman, E. P.; Kyle, K. R.; Moore, C. B.; Bergman, R. G. *J. Am. Chem. Soc.* **1994**, *116*, 7369–7377. (b) Bengali, A. A.; Schultz, R. H.; Moore, C. B.; Bergman, R. G. *J. Am. Chem. Soc.* **1994**, *116*, 9585–9589. (c) McNamara, B. K.; Yeston, J. S.; Bergman, R. G.; Moore, C. B. *J. Am. Chem. Soc.* **1999**, *121*, 6437–6443.

(2) (a) Slone, C. S.; Weinberger, D. A.; Mirkin, C. A. *Prog. Inorg. Chem.* **1999**, *48*, 233–350. (b) Braunstein, P.; Naud, F. *Angew. Chem., Int. Ed.* **2001**, *40*, 680–699.

(3) La Placa, S. J.; Ibers, J. A. *Inorg. Chem.* **1965**, *4*, 778–783.

(4) Brookhart, M.; Green, M. L. H.; Wong, L.-L. *Prog. Inorg. Chem.* **1988**, *36*, 1–124.

(5) Brookhart, M.; Green, M. L. H.; Parkin, G. *Proc. Natl. Acad. Sci. U.S.A.* **2007**, *104*, 6908–6914.

(6) Sato, M.; Tatsumi, T.; Kodama, T.; Hidai, M.; Uchida, T.; Uchida, Y. *J. Am. Chem. Soc.* **1978**, *100*, 4447–4452.

(7) Muir, K. W.; Ibers, J. A. *Inorg. Chem.* **1970**, *9*, 440–447.

(8) Otsuka, S.; Yoshida, T.; Matsumoto, M.; Nakatsu, K. *J. Am. Chem. Soc.* **1976**, *98*, 5850–5858.

(9) King, W. A.; Luo, X.-L.; Scott, B. L.; Kubas, G. J.; Zilm, K. W. *J. Am. Chem. Soc.* **1996**, *118*, 6782–6783.

10.1021/om800401d CCC: $40.75
Publication on Web 07/12/2008

weakly to the Mo.[10] The C═C ligand is readily displaced by other ligands, so that the η^3-PPh_3 ligand functions as a hemilabile ligand. In this paper we report the synthesis, characterization, and structure of $[Cp(CO)_2(\eta^3\text{-}PPh_3)Mo]^+[BAr'_4]^-$, along with $[Cp(CO)_2(PPh_3)Mo(ICH_3)]^+$ and $[Cp(CO)_2(PPh_3)Mo(OH_2)]^+$, in which an ICH_3 or H_2O ligand has displaced the weakly bound C═C interaction. Computational studies provide further insights into the nature of the weak bonding.

Results and Discussion

Synthesis and Spectroscopic Characterization of an η^3-PPh_3 Complex: Different Products Resulting from Different Counterions. Commonly used anions such as BF_4^- and PF_6^- were classically considered noncoordinating, but are now known to bind to some metal cations through the F atom.[11] Observation and characterization of very weak bonding interactions in cationic metal complexes requires the use of even more weakly coordinating counterions. A variety of very weakly coordinating anions[12] have become available and have had an impact in many homogeneous catalytic reactions, especially olefin polymerizations.[13] Beck and co-workers reported the synthesis of many metal carbonyl complexes with coordinated BF_4^-, PF_6^-, and related weakly coordinating anions.[11] Hydride transfer from $Cp(CO)_2(PPh_3)MoH$ to $Ph_3C^+BF_4^-$ gives $Cp(CO)_2(PPh_3)MoFBF_3$[14] (eq 1). We measured the kinetics of this and several related hydride transfer reactions using stopped-flow techniques.[15,16] When the reaction is carried out at −80 °C and monitored by ^1H NMR, a 90:10 mixture of *trans*-$Cp(CO)_2(PPh_3)MoFBF_3$ and $[trans\text{-}Cp(CO)_2(PPh_3)Mo(ClCH_2Cl)]^+BF_4^-$ was initially observed. When the temperature is raised, the weakly coordinating dichloromethane ligand is displaced, and the thermodynamically favored product *cis*-$Cp(CO)_2(PPh_3)MoFBF_3$ forms cleanly.

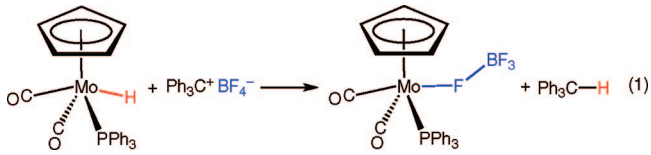

(1)

A completely different product results when hydride abstraction from $Cp(CO)_2(PPh_3)MoH$ is carried out using a much more weakly coordinating counterion (eq 2). Reaction of $Ph_3C^+BAr'_4^-$ with $Cp(CO)_2(PPh_3)MoH$ at −30 °C led to the isolation of a new complex, $[Cp(CO)_2(\eta^3\text{-}PPh_3)Mo]^+[BAr'_4]^-$, in 84% yield. The IR spectrum of the isolated product exhibited bands for the metal carbonyl stretches at 2009 and 1939 cm^{-1}. As shown in Table 1, the bands of the product are shifted to even higher energy than in $Cp(CO)_2(PPh_3)MoFBF_3$, indicating lower electron density at the metal in the new product. Table 1 also lists ν(CO) bands of related compounds for comparison. All of these cationic complexes have ν(CO) bands at higher energy than those of the neutral hydride $Cp(CO)_2(PPh_3)MoH$ (1936, 1855 cm^{-1} in CH_2Cl_2).

Table 1. ν(CO) IR Data in CH_2Cl_2 Solution for Mo Complexes with Weakly Coordinating Ligands

complex	ν(CO), cm^{-1}	ref
$[Cp(CO)_2(\eta^3\text{-}PPh_3)Mo]^+BAr'_4^-$	2009, 1939	this work
$[Cp(CO)_2(PPh_3)Mo(ICH_3)]^+BAr'_4^-$	1987, 1917	this work
$[Cp(CO)_2(PPh_3)Mo(OH_2)]^+BAr'_4^-$	1985, 1909	this work
$[Cp(CO)_2(PPh_3)Mo(O{=}CEt_2)]^+BAr'_4^-$	1992, 1910	17
$Cp(CO)_2(PPh_3)MoFBF_3$	1989, 1905	15

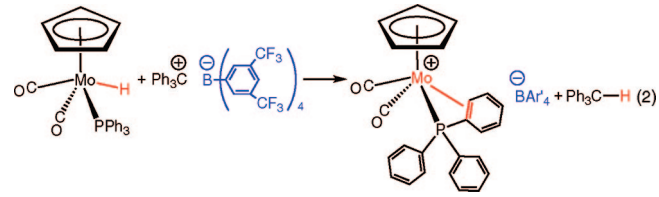

(2)

The ^1H NMR spectrum of the product is not very informative at room temperature; a single Cp resonance indicated a pure product, but the aromatic region exhibited multiplets for the aromatic protons of the PPh_3 ligand. An NMR spectrum at −60 °C, however, shows a triplet (J = 6.9 Hz) at δ 6.12, which integrates for one proton. Homonuclear decoupling of the aromatic resonances at δ 7.4 results in the collapse of this triplet to a doublet. We assign this resonance to one ortho CH on *one* of the three phenyl groups of the PPh_3 ligand, with the triplet pattern being accounted for by $^3J_{HH} \approx {}^3J_{PH}$. This suggests that one of the Ph rings has a substituent that interacts with the Mo. Two plausible bonding configurations are coordination of one of the C═C bonds of a phenyl ring to the Mo as shown in eq 2, and interaction of an ortho C−H bond of the phenyl ring to the Mo in an agostic bond,[4,5] as shown in Figure 1. While the triplet observed in the low-temperature ^1H NMR is consistent with either of these two structural possibilities, the ^{13}C NMR spectrum at −60 °C has two resonances that are informative in distinguishing between the two structures under consideration. Since the specific bonding of a C═C of one of the Ph rings renders the other two Ph rings inequivalent, a large number of resonances are found between δ 120 and 135 in the aromatic region of the ^{13}C NMR spectrum. A doublet (J_{CP} = 29 Hz) at δ 81.5 and a doublet (J_{CP} = 12 Hz) at δ 90.0 are assigned as the ipso and ortho carbons of one of the C═C bonds of the Ph ring. These two resonances are observed in the ^{13}C NMR spectrum at chemical shifts more consistent with coordinated alkenes than a normal aromatic carbon. These data favor the structure shown in eq 2, in which one C═C bond is coordinated to the Mo, rather than the agostic structure involving one C−H of the phenyl ring (Figure 1).

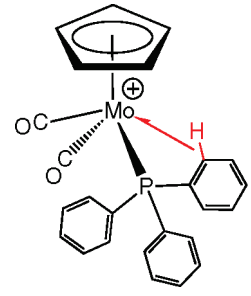

Figure 1. Possible agostic structure for $[Cp(CO)_2(PPh_3)Mo]^+[BAr'_4]^-$.

(10) For a preliminary communication of these results, see: Cheng, T.-Y.; Szalda, D. J.; Bullock, R. M. *J. Chem. Soc., Chem. Commun.* **1999**, 1629–1630.
(11) Beck, W.; Sünkel, K. *Chem. Rev.* **1988**, *88*, 1405–1421.
(12) (a) Strauss, S. H. *Chem. Rev.* **1993**, *93*, 927−942. Reed, C. A. *Acc. Chem. Res.* **1998**, *31*, 133–139. (b) Krossing, I.; Raabe, I. *Angew. Chem., Int. Ed.* **2004**, *43*, 2066–2090.
(13) Chen, E. Y.-X.; Marks, T. J. *Chem. Rev.* **2000**, *100*, 1391–1434.
(14) Sünkel, K.; Ernst, H.; Beck, W. *Z. Naturforsch.* **1981**, *36b*, 474–481.
(15) Cheng, T.-Y.; Brunschwig, B. S.; Bullock, R. M. *J. Am. Chem. Soc.* **1998**, *120*, 13121–13137.
(16) (a) Cheng, T.-Y.; Bullock, R. M. *J. Am. Chem. Soc.* **1999**, *121*, 3150–3155. (b) Cheng, T.-Y.; Bullock, R. M. *Organometallics* **2002**, *21*, 2325–2331.

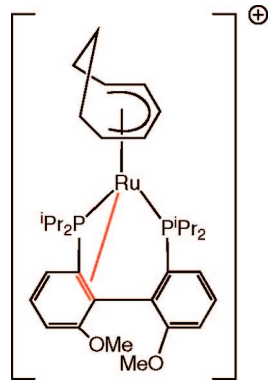

Figure 2. C═C bonded to Ru in [(MeO-BIPHEP)Ru(η^5-C$_8$H$_{11}$)]$^+$.

Further support for our assignment of C═C bonding to the metal comes from a comparison with complexes that exhibit a similar interaction with a diphosphine. Pregosin and co-workers reported detailed NMR studies of a series of cationic Ru complexes that were shown to have a six-electron-donor diphosphine ligand, with one C═C bond coordinated from an arene ring.[18] 2D NMR studies of [(MeO-BIPHEP)Ru(η^5-C$_8$H$_{11}$)]$^+$ provided further characterization of the bonding shown in Figure 2. The ^{13}C NMR resonances of the coordinated C═C atoms appear at δ 74.5 and 95.1 and are distinctly upfield of the analogous carbons in the other ring that are not coordinated (δ 139.7 and 135.4). The resonances for the bound C═C in their Ru complex appear at a similar chemical shift to those in [Cp(CO)$_2$(PPh$_3$)Mo]$^+$. Structural studies of closely related Ru complexes show that the angle between the two aryl rings distorts, facilitating the bonding by allowing the π-system to come closer to the metal. Similar bonding of a C═C of an arene ring of a diphosphine was found in CpRu[(R)-(BINAP)]$^+$I.[19]

Crystal Structure of [Cp(CO)$_2$(η^3-PPh$_3$)Mo]$^+$[BAr′$_4$]. Crystallography of [Cp(CO)$_2$(η^3-PPh$_3$)Mo]$^+$[BAr′$_4$]$^-$ was carried out at the National Synchrotron Light Source, where the high intensity of X-rays available enabled us to determine the crystal structure of the small (0.02 × 0.08 × 0.08 mm) crystal available. The use of weakly coordinating counterions[12] has been very beneficial in recent years, enabling the synthesis of complexes that could not be obtained with traditional counterions and enhancing some catalytic reactions. In some cases complexes with such counterions may not easily form crystals that are well-suited for X-ray diffraction, so the use of a high-intensity source of X-rays can ameliorate these limitations by allowing reliable structural determinations from small crystals.

The ORTEP diagram shown in Figure 3 shows the η^3-PPh$_3$ bonding to the Mo, and Table 2 lists selected bond distances and angles. The distances from Mo to the two carbons in the C═C bond are long: Mo−C(31) = 2.566(9) Å and Mo−C(32) = 2.645(9) Å. Two other complexes with η^3-PPh$_3$ ligands that have been crystallographically characterized also show a disparity in the M−C distances, with the distance to the ipso carbon being shorter than that to the ortho carbon. The rhodium cation

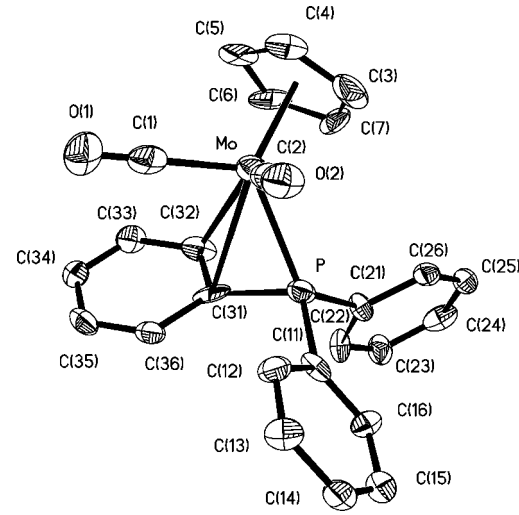

Figure 3. ORTEP diagram (30% probability ellipsoids) of [Cp(CO)$_2$(η^3-PPh$_3$)Mo]$^+$ (hydrogen atoms not shown).

Table 2. Selected Bond Distances (Å) and Angles (deg) for [Cp(CO)$_2$(η^3-PPh$_3$)Mo]$^+$

Bond Distances		Bond Angles	
Mo−C(2)	1.968(12)	C(2)−Mo−C(1)	79.7(5)
Mo−C(1)	1.99(2)	C(2)−Mo−P	83.8(3)
Mo−P	2.429(3)	C(1)−Mo−P	115.7(3)
Mo−C(31)	2.566(9)	P−Mo−C(31)	42.1(2)
Mo−C(32)	2.645(9)	P−Mo−C(32)	65.5(2)
C(31)−C(32)	1.418(13)	Mo−P−C(31)	73.0(3)
C(31)−C(36)	1.445(14)	Mo−P−C(21)	117.8(3)
C(32)−C(33)	1.424(14)	Mo−P−C(11)	131.3(4)
C(33)−C(34)	1.361(14)		
C(34)−C(35)	1.404(13)		
C(35)−C(36)	1.368(13)		

Rh(PPh$_3$)$_3$$^+$ has one of the three PPh$_3$ ligands bound as η^3; the structure was determined for the ClO$_4$$^-$ salt[20] and with a carborane anion.[21] The latter has Rh−C distances of 2.502(8) and 2.611(9) Å, while those in CpRu(η^3-PPh$_3$)(PMe^{i}Pr$_2$)$^+$ are shorter,[22] 2.371(3) and 2.459(3) Å. The expected M−C distances will depend on the metal, but for all three of these complexes having an η^3-PPh$_3$ ligand, the M−C distances are long, compared to M−C distances in the range of about 2.1−2.25 Å for Cp*(PMe$_3$)Rh(η^2-phenanthrene),[23] Cp*(NO)Ru(η^2-naphthalene),[24] [(NH$_3$)$_5$Os(η^2-naphthalene)]$^{2+}$,[25] and [κ^2-(Hpz*)BHpz*$_2$]Pt(H)(η^2-benzene)]$^+$,[26] in which the arene is bonded η^2 to the metal but is not bonded to a phosphine.

In the two Ph rings that do not interact with the Mo, the average carbon−carbon bond length was 1.39(1) Å, while in the coordinated ring there is a pattern of alternating long and short bond lengths (see Table 2), indicating some localization. The long bonds average 1.42 Å, and two of the short bonds

(17) Bullock, R. M.; Voges, M. H. *J. Am. Chem. Soc.* **2000**, *122*, 12594–12595. (a) Voges, M. H.; Bullock, R. M. *J. Chem. Soc., Dalton Trans.* **2002**, 759–770.

(18) (a) Feiken, N.; Pregosin, P. S.; Trabesinger, G.; Scalone, M. *Organometallics* **1997**, *16*, 537–543. (b) Feiken, N.; Pregosin, P. S.; Trabesinger, G.; Albinati, A.; Evoli, G. L. *Organometallics* **1997**, *16*, 5756–5762. (c) Geldbach, T. J.; Pregosin, P. S. *Eur. J. Inorg. Chem.* **2002**, 1907–1918.

(19) Pathak, D. D.; Adams, H.; Bailey, N. A.; King, P. J.; White, C. *J. Organomet. Chem.* **1994**, *479*, 237–245.

(20) Yared, Y. W.; Miles, S. L.; Bau, R.; Reed, C. A. *J. Am. Chem. Soc.* **1977**, *99*, 7076–7078.

(21) Knobler, C. B.; Marder, T. B.; Mizusawa, E. A.; Teller, R. G.; Long, J. A.; Behnken, P. E.; Hawthorne, M. F. *J. Am. Chem. Soc.* **1984**, *106*, 2990–3004.

(22) Jiménez-Tenorio, M.; Puerta, M. C.; Valerga, P. *Organometallics* **2002**, *21*, 628–635.

(23) Chin, R. M.; Dong, L.; Duckett, S. B.; Partridge, M. G.; Jones, W. D.; Perutz, R. N. *J. Am. Chem. Soc.* **1993**, *115*, 7685–7695.

(24) Tagge, C. D.; Bergman, R. G. *J. Am. Chem. Soc.* **1996**, *118*, 6908–6915.

(25) Winemiller, M. D.; Kelsch, B. A.; Sabat, M.; Harman, W. D. *Organometallics* **1997**, *16*, 3672–3678.

(26) Reinartz, S.; White, P. S.; Brookhart, M.; Templeton, J. L. *J. Am. Chem. Soc.* **2001**, *123*, 12724–12725.

average 1.36(1) Å. The C═C bonded to the metal is elongated to 1.42(1) Å.

There are 18 F···H distances in the range 2.6−3.0 Å between C−H bonds (of the Ph and Cp rings) and C−F bonds of the anion in $[Cp(CO)_2(\eta^3\text{-}PPh_3)Mo]^+[BAr'_4]^-$, possibly indicating weak C−F···H−C hydrogen bonding interactions. There are 15 F···H distances in this range in $[Cp(CO)_2(PPh_3)Mo(OH_2)]^+BAr'_4{}^-$, and 11 were found in $[Cp(CO)_2(PPh_3)Mo(ICH_3)]^+BAr'_4{}^-$ (*vide infra*). The presence of C−F···H−C interactions has been previously recognized in organometallic complexes[27] and in numerous organic compounds such as fluorobenzenes.[28] Surveys and analyses of crystallographic data have been reported,[29,30] and theoretical studies have also examined the C−F···H−C interaction.[31] Even though such interactions are individually weak, collectively they can have an influence on the crystal structure. The assignment of these weak interactions as hydrogen bonds,[32] however, remains controversial.[30]

Comparison of PPh_3 Ligands Containing C═C Bonds to the Metal with Those Having an Agostic C−H Interaction. In thousands of organometallic complexes, PPh_3 functions as a simple two-electron donor through the phosphorus. Of those that have an additional interaction, there appears to be a much higher prevalence of C−H agostic interactions compared to weakly bound C═C bonds. We now consider structural features that clearly distinguish between the two modes of bonding. La Placa and Ibers reported evidence for a possible interaction between the Ru and the H on the ortho carbon of one of the Ph rings in the crystal structure of $RuCl_2(PPh_3)_3$[3] (Chart 1). They cautiously interpreted the evidence for this interaction as being "extremely tenuous", but subsequent studies of other complexes have provided further support for the three-center, two-electron agostic[4,5] bonding. Hidai and co-workers reported the structure of a Mo carbonyl complex where a chelating diphosphine exhibited this type of interaction[6] (Chart 1). Kubas and co-workers reported detailed NMR characterization of the agostic C−H interaction in the closely related complexes $Mo(CO)[(PhCH_2)_2PCH_2CH_2P(CH_2Ph)_2]_2$.[33]

Multiple agostic interactions to a single metal can occur, as documented by the crystal structure of $Pd(P^tBu_2Ph)_2$ which showed that two C−H bonds of Ph rings were within agostic bonding distance of the Pd, along with similar weak interactions with ^{t}Bu substituents on the ligand[8] (Chart 1). Kubas and co-workers found that the crystal structure of $Mn(CO)(Ph_2PCH_2CH_2PPh_2)_2^+$ had two agostic interactions to the same metal, arising from different C−H bonds of different Ph rings.[9]

Diagnostic structural features of complexes exhibiting C−H agostic interactions distinguish them from complexes having C═C bonding of the η^3-PPh_3 ring. A conspicuous difference in the structures of complexes exhibiting the two different types

Chart 1. Complexes Having Agostic C−H Interactions of P−Ph Groups

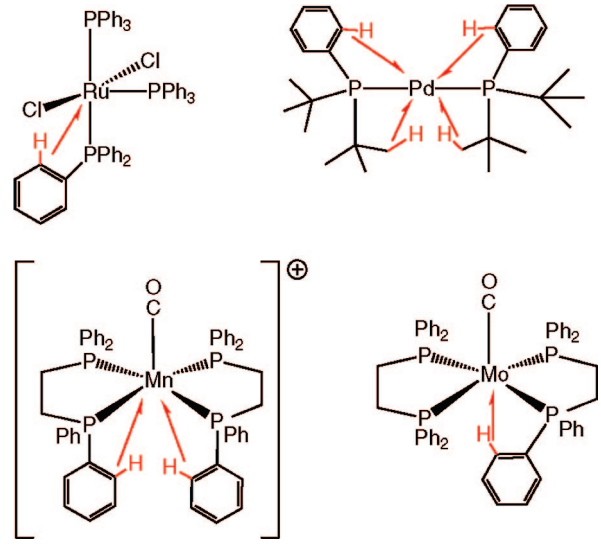

of bonding is the location of the metal compared to the plane of the interacting Ph ring. Since the η^3-PPh_3 bonding uses the p-orbitals of the C═C fragment of the Ph ring, the metal resides above the plane of the ring. For $[Cp(CO)_2(\eta^3\text{-}PPh_3)Mo]^+[BAr'_4]^-$, an angle of 62.1° is found for the dihedral angle between the plane of the Ph ring and the plane containing the metal and the two interacting (C═C) carbons. This angle is similar to the dihedral angles in $[Rh(PPh_3)_3]^+$ and $CpRu(\eta^3\text{-}PPh_3)(PMe^iPr_2)^+$, which were shown by crystallography to have an η^3-PPh_3 ligand (Table 3). These values are also similar to transition metal complexes having η^2-arene ligands that are *not* constrained in their geometry by being bound to a phosphine, such as the dihedral angle of 71.1° for $Cp^*(PMe_3)Rh(\eta^2\text{-phenanthrene})$,[23] 71.1° for $Cp^*(NO)Ru(\eta^2\text{-naphthalene})$,[24] 71.8° for $[(NH_3)_5Os(\eta^2\text{-naphthalene})]^{2+}$,[25] and 73.0° for $[\kappa^2\text{-}(Hpz^*)BHpz^*_2]Pt(H)(\eta^2\text{-benzene})]^+$[26] (pz* = 3,5-dimethylpyrazolyl). In contrast, complexes containing an agostic C−H bond of the P−Ph moiety have the metal nearly in the plane of the ring, with dihedral angles in the range 0−20°.

In addition to these striking differences in dihedral angles, there is also a notable difference in the $M-P-C_{ipso}$ angles (Table 3). The acute M−P−C angles of 70−76° for the η^3-PPh_3 ligands contrast with the much less distorted angles observed with the complexes having an agostic C−H interaction, which are generally >107°. For comparison, the Rh−P−C angles for the noninteracting Ph groups in $[Rh(PPh_3)_3]^+$ are 123.3(4)° and 126.2(3)°.[21] The Mo−P−C angle in $[Cp(CO)_2(\eta^3\text{-}PPh_3)Mo]^+$ is smaller than the Mo−P−C angle of 87.4(1)° of $CpMo(\eta^2\text{-}C_6H_4PMe_2)(PMe_2Ph)$, a complex in which the phosphine is ortho-metalated.[34]

The M···H distance is often used in consideration of possible agostic interactions.[4,5] In most cases these distances are inferred on the basis of the heavy atom positions, since hydrogen atom positions are usually not reliably located using X-ray diffraction. The complexes in Table 3 with η^3-PPh_3 bonding have shorter M···H distances than those with agostic interactions, which fall in the range of about 2.7−3.0 Å. The bonding in $[Rh(PPh_3)_3]^+$ has been suggested to be agostic,[4] but we believe that the criteria of dihedral angles and the M−P−C angles as

(27) (a) Brammer, L.; Klooster, W. T.; Lemke, F. R. *Organometallics* **1996**, *15*, 1721–1727. (b) Teff, D. J.; Huffman, J. C.; Caulton, K. G. *Inorg. Chem.* **1997**, *36*, 4372–4380.

(28) Thalladi, V. R.; Weiss, H.-C.; Blaser, D.; Boese, R.; Nangia, A.; Desiraju, G. R. *J. Am. Chem. Soc.* **1998**, *120*, 8702–8710.

(29) (a) Shimoni, L.; Glusker, J. P. *Struct. Chem.* **1994**, *5*, 383–397. (b) Brammer, L.; Bruton, E. A.; Sherwood, P. *Cryst. Growth Des.* **2001**, *1*, 277–290.

(30) (a) Dunitz, J. D.; Taylor, R. *Chem.−Eur. J.* **1997**, *3*, 89–98. (b) Howard, J. A. K.; Hoy, V. J.; O'Hagan, D.; Smith, G. T. *Tetrahedron* **1996**, *52*, 12613–12622.

(31) Hyla-Kryspin, I.; Haufe, G.; Grimme, S. *Chem.−Eur. J.* **2004**, *10*, 3411–3422.

(32) Desiraju, G. R.; Steiner, T. *The Weak Hydrogen Bond in Structural Chemistry and Biology*; Oxford University Press: Oxford, 1999.

(33) Luo, X.-L.; Kubas, G. J.; Burns, C. J.; Eckert, J. *Inorg. Chem.* **1994**, *33*, 5219–5229.

(34) Poli, R.; Krueger, S. T.; Abugideiri, F.; Haggerty, B. S.; Rheingold, A. L. *Organometallics* **1991**, *10*, 3041–3046.

Table 3. Comparison of Dihedral Angles, M−P−C_{ipso} Angles and M···H Distances for Complexes with η^3-PPh_3 or C−H Agostic P−Ph Ligands

complex	dihedral angle MCC/arene (deg)[a]	M−P−C (deg)	M···H (Å)[b]	ref
		Complexes with η^3-PPh_3 Ligands		
$[Cp(CO)_2(\eta^3\text{-}PPh_3)Mo]^+$	62.1	73.0(3)	2.64	this work
$[Rh(PPh_3)_3]^+$	59.0	75.6(3)	2.57	21
$CpRu(\eta^3\text{-}PPh_3)(PMe^iPr_2)^+$	58.2	69.56(10)	2.68	22
		Complexes with C−H Agostic P−Ph Ligands		
$Pd(PPh^tBu_2)_2$	10	113.1(3)	2.83(11)	8
$RhHCl(SiCl_3)(PPh_3)_2$	9.7	107−121	2.8	7
$RuCl_2(PPh_3)_3$	0.60	100−128	2.7[c]	3
$Mo(CO)(Ph_2PCH_2CH_2PPh_2)_2$	20.3	108.9	2.98(11)	6
$Mn(CO)[Ph_2PCH_2CH_2PPh_2]_2^+$	3.0, 4.8	112.4, 115.1	2.89(6),2.98(6)	9

[a] Dihedral angle between the plane of the Ph ring and the plane containing the metal and the two interacting (C═C) carbons. [b] The M···H separation is the distance between the metal and the H on the ortho carbon of the arene ring. In most cases such distances are calculated and are subject to inaccuracies of locating H atoms from X-ray diffraction. [c] The value of >2.7 Å for the M···H distance in $RuCl_2(PPh_3)_3$ is our estimate. La Placa and Ibers reported[3] a M···H distance of 2.59 Å based on a rigid group refinement for the Ph ring, using a C−H bond length of 1.08 Å. In modern structural studies, the individual carbon atoms would be refined, and a 0.95 Å C−H bond length would be used, which would give a M···H distance estimated as >2.7 Å.

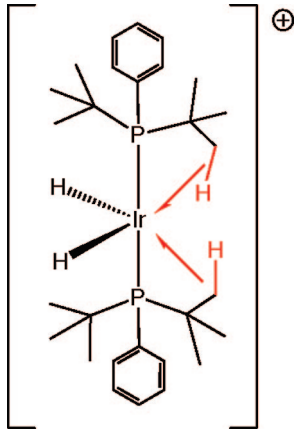

Figure 4. An Ir complex that has two agostic C−H interactions but no C═C (phenyl) bonds to Ir.

documented in Table 3 provide a more conclusive criterion of the predominant bonding, rather than using the M···H distances to distinguish between the two bonding modes. The H on the ortho carbon of the Ph ring is drawn close to the metal by the geometrical requirements of the η^3-PPh_3 bonding, so we consider the relatively short M···H distances to be an inevitable consequence of the η^3-PPh_3 bonding, rather than independent evidence of an agostic interaction.

Caulton and co-workers reported extensive experimental and computational studies on agostic interactions in a series of cationic Ir complexes.[35] As shown in Figure 4, $Ir(H)_2(P^tBu_2Ph)_2^+$ has agostic interactions involving C−H bonds from different ^{t}Bu groups on two different phosphines. Bond distances for the Ir−C bonds involved in these agostic interactions range from 2.81 to 2.94 Å. This agostic interaction with an aliphatic C−H is observed in preference to agostic (or C═C) bonding involving the Ph ring; Ir···C(phenyl) separations were at least 3.48 Å. Structural and computational studies on related complexes showed how sensitive the agostic interactions can be to steric effects. The ortho-metalated complex $IrH(\eta^2\text{-}C_6H_4P^tBu_2)(P^tBu_2Ph)_2^+$ has only one agostic interaction (again with a C−H bond of a ^{t}Bu group) even though it had two vacant coordination sites. A related complex with P^iPr groups, $Ir(H)_2(P^iPr_2Ph)_3^+$, has no agostic interactions and is stable in a 16-electron configuration. Caulton and co-workers concluded from these studies that steric pressure can encourage the formation of agostic interactions by forcing the appropriate C−H bond close enough to the metal to facilitate the formation of an agostic bond. We have carried out computations (*vide infra*) on the hypothetical complex $[Cp(CO)_2(PH^tBuPh)Mo]^+$. This complex is related to $[Cp(CO)_2(\eta^3\text{-}PPh_3)Mo]^+$, but it has a chance to form an aliphatic agostic bond that might compete with arene bonding.

Weak bonding of metals to C═C bonds is not limited to aromatic rings of phosphines: we found that a C═C bond of a mesityl group in an N-heterocyclic carbene ligand is weakly bound to the tungsten in $CpW(CO)_2(IMes)^+B(C_6F_5)_4^-$ (IMes = 1,3-bis(2,4,6-trimethylphenyl)imidazol-2-ylidene).[36] This W complex catalyzes the hydrogenation[36] and hydrosilylation[37] of ketones.

Computational Studies on $[Cp(CO)_2(PPh_3)Mo]^+$ and $[Cp(CO)_2(PH_2Ph)Mo]^+$. B3LYP hybrid DFT[38] and *ab initio* second-order Møller−Plesset perturbation theory (MP2)[39] computations, with the Gaussian 03 package of programs using the Los Alamos ECP plus DZ basis[40] for Mo and Nb, and the 6-31G(d,p) basis[41] for all other elements, were carried out on $[Cp(CO)_2(PPh_3)Mo]^+$ and on the hypothetical complex $[Cp(CO)_2(PH_2Ph)Mo]^+$ to provide further understanding of the factors influencing the bonding mode. We sought to determine if steric pressure exerted by two Ph groups was necessary for the formation of the bonding of the C═C to the metal. B3LYP calculations were carried out on the hypothetical complexes $[Cp(CO)_2(PH^tBuPh)Mo]^+$ and $[Cp(CO)_2(PH_2Ph)Nb]^0$ to address the competition between agostic vs arene bonding and the effect of the charge on the metal center.

(35) (a) Cooper, A. C.; Streib, W. E.; Eisenstein, O.; Caulton, K. G. *J. Am. Chem. Soc.* **1997**, *119*, 9069–9070. (b) Ujaque, G.; Cooper, A. C.; Maseras, F.; Eisenstein, O.; Caulton, I. G. *J. Am. Chem. Soc.* **1998**, *120*, 361–365. (c) Cooper, A. C.; Clot, E.; Huffman, J. C.; Streib, W. E.; Maseras, F.; Eisenstein, O.; Caulton, K. G. *J. Am. Chem. Soc.* **1999**, *121*, 97–106.

(36) (a) Dioumaev, V. K.; Szalda, D. J.; Hanson, J.; Franz, J. A.; Bullock, R. M. *Chem. Commun.* **2003**, 1670–1671. (b) Wu, F.; Dioumaev, V. K.; Szalda, D. J.; Hanson, J.; Bullock, R. M. *Organometallics* **2007**, *26*, 5079–5090.

(37) Dioumaev, V. K.; Bullock, R. M. *Nature* **2003**, *424*, 530–532.

(38) (a) Becke, A. D. *J. Chem. Phys.* **1993**, *98*, 5648–5652. (b) Lee, C. T.; Yang, W. T.; Parr, R. G. *Phys. Rev. B* **1988**, *37*, 785–789. (c) Becke, A. D. *Phys. Rev. A* **1988**, *38*, 3098–3100.

(39) (a) Møller, C.; Plesset, M. S. *Phys. Rev.* **1934**, *46*, 618–622. (b) Head-Gordon, M.; Pople, J. A.; Frisch, M. J. *Chem. Phys. Lett.* **1988**, *153*, 503–506.

(40) Hay, P. J.; Wadt, W. R. *J. Chem. Phys.* **1985**, *82*, 270–283.

(41) Ditchfield, R.; Hehre, W. J.; Pople, J. A. *J. Chem. Phys.* **1971**, *54*, 724–728.

Table 4. Bond Distances (Å) and Angles (deg) from the Computed Structures of $[Cp(CO)_2(PPh_3)Mo]^+$ and $[Cp(CO)_2(PH_2Ph)Mo]^+$ (B3LYP and MP2)

$[Cp(CO)_2(PPh_3)Mo]^+$			$[Cp(CO)_2(PH_2Ph)Mo]^+$	
B3LYP	MP2[a]	parameter[b]	B3LYP	MP2[c]
2.48	2.50	Mo−P	2.44	2.45
2.69	2.74	Mo−C_{ipso}	2.72	2.73
2.82	2.90	Mo−C_{ortho}	2.97	2.94
75.8	76.9	Mo−P−C_{ipso}	78.1	78.0
60.7	61.5	dihedral angle[d]	60.1	61.1

[a] Orbitals 98 through 518 and the 20 electrons occupying orbitals 98 through 107 were included in the correlation energy calculation. [b] C_{ipso} = C(31) and C_{ortho} = C(32) in $[Cp(CO)_2(\eta^3\text{-}PPh_3)Mo]^+$ (Figure 3). [c] Orbitals 59 through 310 and the 18 electrons occupying orbitals 59 through 67 were included in the correlation energy calculation. [d] Dihedral angle between the plane of the Mo and the ipso and ortho carbon atoms of the arene ring and the plane defined by the ipso, ortho, and meta carbon atoms of the arene ring. This convention for defining dihedral angles by four atoms is in widespread use in quantum chemistry codes and should correspond quite closely to the crystallographic convention employing the dihedral angle between the plane of the Ph ring and the plane containing the metal and the two interacting (C═C) carbons, since deviations of the Ph ring from nonplanarity are very small (±0.015 Å).

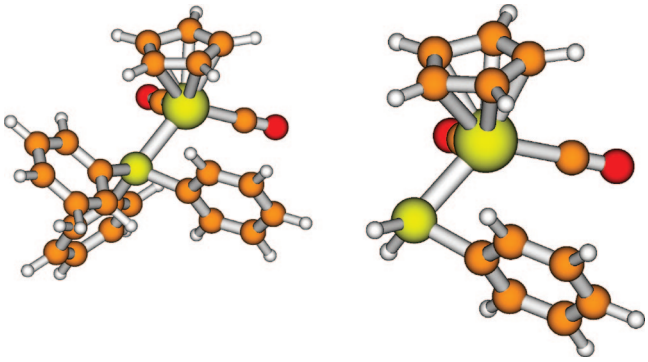

Figure 5. Structures of $[Cp(CO)_2(PPh_3)Mo]^+$ (left) and $[Cp(CO)_2(PH_2Ph)Mo]^+$ (right) computed by MP2.

The features of the computed minimized structures are similar to those found experimentally in the crystallographic study. Our experimental and computational values are also similar to those computed recently by Costa, Calhorda, and Pregosin using the Amsterdam Density Functional program.[42] Metrical parameters are provided in Table 4, and Figure 5 shows the geometry for both complexes. Both have bonding of the C═C of the Ph ring to the Mo. The B3LYP bond distances are (unexpectedly not longer, but) generally shorter than those from the MP2 calculation, although both sets of calculated bond lengths are longer than the experimental values by 0.05 to 0.25 Å. The larger distance of the Mo to the ortho carbon compared to the ipso carbon is also found in the computed structure. The calculated M−P−C angle is within 4° of the experimental value, and it has a very similar value in both $[Cp(CO)_2(PPh_3)Mo]^+$ and the hypothetical $[Cp(CO)_2(PH_2Ph)Mo]^+$ complex which should exhibit no steric pressure to force this angle to be so small (78°). This demonstrates that the arene bonding interaction is sufficiently strong to distort the Mo−P−C angle. While the Mo−P−C angle of the phenyl group involved in the arene interaction in $[Cp(CO)_2(PPh_3)Mo]^+$ is 76°, the other two Mo−P−C angles are 120° and 129°. In $[Cp(CO)_2(PH_2Ph)Mo]^+$, the M−P−C angle is 78°, while the two Mo−P−H angles are 127° and 128°.

(42) Costa, P. J.; Calhorda, M. J.; Pregosin, P. S. *Collect. Czech. Chem. Commun.* **2007**, *72*, 703–714.

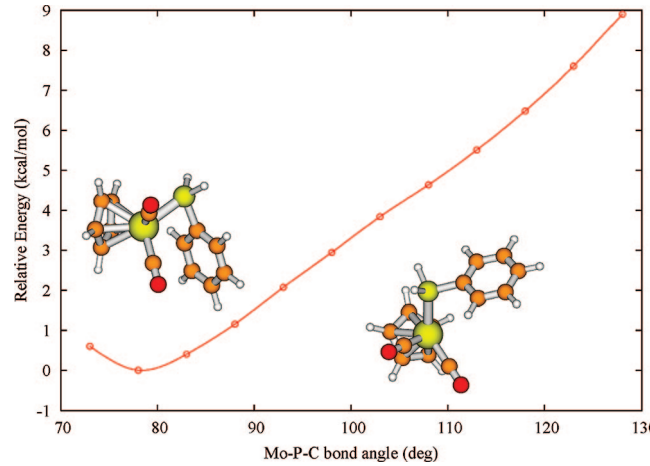

Figure 6. Computed DFT/B3LYP energy of $[Cp(CO)_2(PH_2Ph)Mo]^+$ as a function of the Mo−P−C angle. At each fixed value of the Mo−P−C angle, all other degrees of freedom were relaxed to minimize the energy. The insets show the optimized structure at the equilibrium geometry (78°) and at 108°. The MCC/arene dihedral angles (see text) are 60° and 42°, respectively.

Considering the much larger M−P−C angle found in agostic structures compared to those adopting bonding to the C═C (Table 3), we wondered whether a larger Mo−P−C angle would favor the agostic C−H over C═C bonding to the metal. To investigate this possibility, a series of calculations was performed in which the Mo−P−C angle was scanned in increments of 5°, from 73° to 128°. At each fixed value of this angle, all other degrees of freedom were relaxed to minimize the energy.

A plot of the energy as a function of Mo−P−C angle is shown in Figure 6. The MCC/arene dihedral angle (between the plane of the Ph ring and the plane containing the metal and the two interacting C═C carbons) changes from 60° at the minimum of the curve to 42° for a Mo−P−C angle of 108°. As mentioned above, Mo−P−C angles greater than 100° are usually associated with C−H agostic bonding, and the very slight inflection in the curve shown in Figure 6 between 103° and 108°, together with the decrease in MCC/arene dihedral angle, might be suggestive of the possible onset of an agostic interaction that slightly stabilizes the molecule in that region. The Mo···C_{ortho} and Mo···H distances relevant to a possible agostic interaction at the 108° bond angle are 4.009 and 3.858 Å, respectively, which are much too large to be considered an agostic interaction. Weak M···H−C interactions have been observed in many complexes at M···H distances longer than those normally found in agostic complexes. Such interactions have been designated as pregostic[43] or preagostic,[44] meaning either that they are on the way to becoming agostic or that they have a weak M···H−C interaction as described by Albinati, Pregosin, and co-workers.[45] A recent review article on agostic interactions favors the term "anagostic" to describe weak hydrogen bonding[46] and other interactions that are not truly agostic.[5]

(43) Bortolin, M.; Bucher, U. E.; Ruegger, H.; Venanzi, L. M.; Albinati, A.; Lianza, F.; Trofimenko, S. *Organometallics* **1992**, *11*, 2514–2521.

(44) (a) Lewis, J. C.; Wu, J.; Bergman, R. G.; Ellman, J. A. *Organometallics* **2005**, *24*, 5737–5746. (b) Zhang, Y.; Lewis, J. C.; Bergman, R. G.; Ellman, J. A.; Oldfield, E. *Organometallics* **2006**, *25*, 3515–3519.

(45) (a) Albinati, A.; Anklin, C. G.; Ganazzoli, F.; Ruegg, H.; Pregosin, P. S. *Inorg. Chem.* **1987**, *26*, 503–508. (b) Albinati, A.; Pregosin, P. S.; Wombacher, F. *Inorg. Chem.* **1990**, *29*, 1812–1817. (c) Albinati, A.; Arz, C.; Pregosin, P. S. *Inorg. Chem.* **1987**, *26*, 508–513.

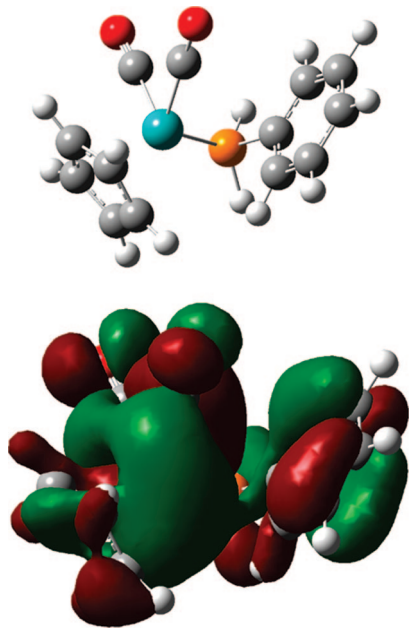

Figure 7. Structural view (top panel) and HOMO (bottom panel) of $[Cp(CO)_2(\eta^3\text{-}PH_2Ph)Mo]^+$ with an isovalue of 0.015 showing the arene bonding to the metal center through overlap of the above-plane π-orbitals of the ipso and ortho carbon atoms of the phenyl ring with a metal d-orbital.

Regardless of the nomenclature of these weak interactions, they normally refer to complexes having M···H distances less than about 3 Å. There was no Mo···H distance found in any of the minimized structures from Figure 6 less than 3 Å, indicating that the interaction of the Mo with the C═C bond of the arene is favored over any type of agostic interaction. When the Mo−P−C angle is opened to 128°, the MCC/arene dihedral angle falls to 26°, but the Mo−C_{ortho} and Mo−H distances are too large (4.461 and 4.140 Å, respectively) for there to be an agostic interaction.

As the Mo−P−C angle opens, changes are also found in the OC−Mo−P angles. At an Mo−P−C angle of 78°, the OC−Mo−P angles are 83.2° and 114.3°; at the larger Mo−P−C angle of 108°, the OC−Mo−P angles are 80.5° and 116.4°.

Figure 7 shows the origin of the relatively weak arene bond to the metal center. It is clear in the figure that the diffuse parts of the above-plane π-orbital of the ipso and ortho carbons of the phenyl ring overlap the diffuse part of a metal d-orbital in a bonding interaction. This interaction requires the proper orientation of the phenyl ring relative to the metal and a sufficiently short distance for the overlap to occur. It may be that these requirements are less demanding than those for an agostic interaction.

Table 5. Calculated Structural Parameters of the $[Cp(CO)_2(PH^tBuPh)Mo]^+$ and $Cp(CO)_2(PH_2Ph)Nb$ Complexes

property	$[Cp(CO)_2(PH^tBuPh)Mo]^+$	$Cp(CO)_2(PH_2Ph)Nb$
M−P (Å)	2.47	2.51
M−C_{ipso} (Å)	2.71	2.90
M−C_{ortho} (Å)	2.81	3.07
M−P−C_{ipso} (Å)	76.8	82.2
MCC/arene dihedral angle (deg)	59.0	58.0
M−H_{tBu} (Å)	3.89	N/A
M−C_{tBu} (Å)	4.32	N/A

Although no definitive evidence for an agostic interaction was obtained in our computations, the energy at the Mo−P−C angle of 108° is about 4.5 kcal/mol higher than that at the Mo−P−C angle of 78° (Figure 6). The energy of the observed interaction between the Mo and the C═C bond would thus be at least 4.5 kcal/mol stronger than the putative agostic interaction. Hoff and co-workers estimated the strength of the agostic interaction in $(CO)_3W(PCy_3)_2$ as 10 ± 6 kcal/mol.[47] A more recent theoretical study of $(CO)_3W(PCy_3)_2$ estimated the strength of the agostic bonds as 7−9 kcal/mol.[48] Taking 8 kcal/mol as representative of an agostic interaction in metal carbonyl complexes, and adding the 4.5 kcal/mol estimated for the difference in the agostic vs C═C bonding to Mo, gives a rough estimate of 12.5 kcal/mol for the strength of the bond between the Mo and the C═C bond in $[Cp(CO)_2(PPh_3)Mo]^+$. This estimate is comparable to the value of 13.4 kcal/mol computed by an energy decomposition analysis of $[Cp(CO)_2(PPh_3)Mo]^+$.[42]

Computational Studies on $[Cp(CO)_2(PH^tBuPh)Mo]^+$ and $Cp(CO)_2(PH_2Ph)Nb$. Introducing a tertiary butyl group in place of one of the hydrogen atoms of the PH_2Ph ligand allows for the possibility of an agostic interaction of a CH_3 group to compete with the arene interaction in the same molecule (cf. Caulton's Ir complex in Figure 4). Figure 8 shows the calculated (DFT/B3LYP) minimum-energy structure of this complex, which exhibits an arene C═C bond but no agostic interaction to a C−H on either the ^{t}Bu or the Ph ring. Table 5 lists the key geometric features.

The three examples in Table 3 with a C═C interaction are cationic complexes, while most of those with an agostic complex are neutral. Considering the relatively small number of examples, this observed trend may not be significant, but we wanted to address the question of the possible dependence of arene bonding on charge by calculating the structure of $Cp(CO)_2(PH_2Ph)Nb$, the neutral Nb analogue of the cationic Mo complex. The computed structure of $[Cp(CO)_2(PH_2Ph)Nb]^0$ in Figure 8 is seen also to exhibit an arene bond, with an acute Nb−P−C angle. The key geometric features of the Nb complex are also listed in Table 5.

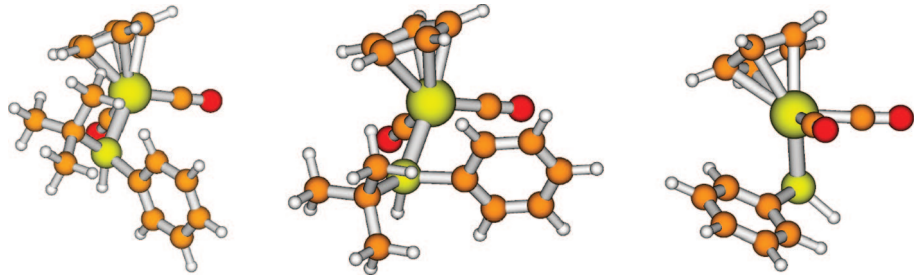

Figure 8. (Left) Starting geometry of $[Cp(CO)_2(PH^tBuPh)Mo]^+$ used when trying to favor an agostic interaction. The Mo···H distance was 2.58 Å for a putative agostic interaction between the Mo and a C−H on the ^{t}Bu group. (Middle) Optimized structure showing that the Mo(C═C) arene bonding is favored over the agostic interaction. (Right) Minimum-energy structure of $[Cp(CO)_2(PH_2Ph)Nb]^0$.

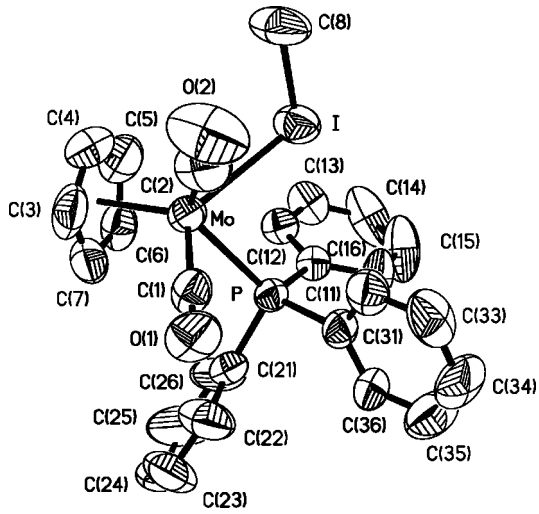

Figure 9. ORTEP diagram (30% probability ellipsoids) of $[Cp(CO)_2(PPh_3)Mo(ICH_3)]^+$ (hydrogen atoms not shown).

Table 6. Selected Bond Distances (Å) and Angles (deg) for $[Cp(CO)_2(PPh_3)Mo(ICH_3)]^+$

Bond Distances		Bond Angles	
Mo−C(1)	1.96(2)	C(2)−Mo−C(1)	73.5(5)
Mo−C(1)	1.967(11)	C(2)−Mo−P	122.4(4)
Mo−P	2.522(3)	C(1)−Mo−P	77.1(3)
Mo−I	2.8592(13)	C(2)−Mo−I	79.2(4)
I−C(8)	2.149(11)	C(1)−Mo−I	125.0(3)
C(1)−O(1)	1.130(11)	P−Mo−I	78.85(7)
C(2)−O(2)	1.15(2)	C(8)−I−Mo	105.7(4)

Displacement of the C═C by Methyl Iodide to Give $[Cp(CO)_2(PPh_3)Mo(ICH_3)]^+$. The weak C═C bond of $[Cp(CO)_2(\eta^3\text{-}PPh_3)Mo]^+$ is readily displaced by other ligands, including weakly binding ligands such as CH_3I. Addition of CH_3I to a solution of $[Cp(CO)_2(\eta^3\text{-}PPh_3)Mo]^+$ results in the formation of *cis*-$[Cp(CO)_2(PPh_3)Mo(ICH_3)]^+$ (eq 3). The equilibrium constant was determined from ^1H and ^{31}P NMR measurements to be $K_{eq} = 5.2 \times 10^2\ M^{-1}$ in CD_2Cl_2 at 22 °C. When the solvent (and volatile CH_3I) is pumped off and the residue is dissolved in CD_2Cl_2, most of the $[Cp(CO)_2(\eta^3\text{-}PPh_3)Mo]^+$ is regenerated.

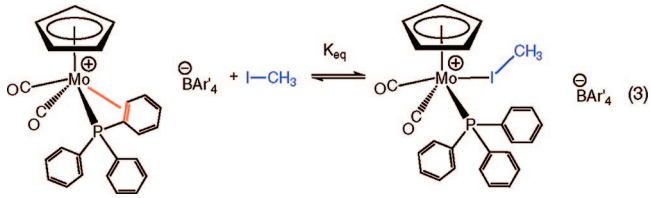

Analytically pure crystals of *cis*-$[Cp(CO)_2(PPh_3)Mo(ICH_3)]^+$ were obtained by addition of excess CH_3I to $[Cp(CO)_2(\eta^3\text{-}PPh_3)Mo]^+$, followed by crystallization at low temperature. The IR spectrum of $[Cp(CO)_2(PPh_3)Mo(ICH_3)]^+$ (Table 1) shows ν(CO) bands at lower energy compared to those for $[Cp(CO)_2(\eta^3\text{-}PPh_3)Mo]^+$, consistent with CH_3I being a stronger donor than the C═C bond. The ^{13}C NMR spectrum of $[Cp(CO)_2(PPh_3)Mo(ICH_3)]^+$ at −60 °C exhibits a doublet ($^3J_{CP} = 4.5$ Hz) at δ −6.0 for the CH_3I ligand, compared to the singlet for free CH_3I, which appears at δ −21.2 under the same conditions. A crystallographic study (Figure 9) shows the cis geometry of the CH_3I and PPh_3 ligands; selected bond distances and angles are given in Table 6. The Mo−I−C angle of 105.7(4)° is quite similar to the Ir−I−C angles of 105.5(4)° and 108.2(5)° found[49] in $[Ir(H)_2(PPh_3)_2(ICH_3)_2]^+$ and the Ru−I−C angle[50] of 104.9(7)° in $[Cp(PPh_3)(CN^tBu)Ru(ICH_3)]^+$. The Mo−I distance in $[Cp(CO)_2(PPh_3)Mo(ICH_3)]^+$, with an ICH_3 ligand, is essentially equal to the Mo−I distance of 2.858(3) Å in the molybdenum iodide complex *trans*-$Cp(CO)_2(PPh_3)MoI$.[51] These distances are also very similar to the Mo−I distance of 2.865(1) Å found in $Cp(CO)_2Mo(\mu\text{-}I)(\mu\text{-}PPh_2)Mn(CO)_4$, in which the iodide bridges a Mo and Mn.[52]

Halogenated hydrocarbons were also once considered to be noncoordinating, but the binding ability of haloalkanes has become well-recognized.[53] Even solvents such as CH_2Cl_2 are now known to be ligands,[54] and structural data have been reported for several chlorocarbon complexes.[55]

Displacement of the C═C by Water to Give $[Cp(CO)_2(PPh_3)Mo(OH_2)]^+$. The C═C ligand of $[Cp(CO)_2(\eta^3\text{-}PPh_3)Mo]^+$ can also be displaced by water to produce the aqua complex $[Cp(CO)_2(PPh_3)Mo(OH_2)]^+$. This complex was first observed as an unintentional side product during preparations of $[Cp(CO)_2(\eta^3\text{-}PPh_3)Mo]^+$. Despite efforts to use rigorously dried solvents and glassware, the formation of aqua complexes occurs in numerous cases. Hughes and co-workers reported the synthesis and crystal structures of a series of Rh and Ir complexes with water ligands.[56] They found that the cationic intermediates $\{Cp^*(PMe_3)M[CF(CF_3)_2]\}^+$ (M = Rh, Ir) are "voracious scavengers of adventitious moisture, even from glass surfaces". Koelle reviewed organometallic aqua complexes,[57] and an extensive compilation of literature references on such complexes is given in a paper by Kubas and co-workers.[58]

(46) Brammer, L. *Dalton Trans.* **2003**, 3145–3157.
(47) Gonzalez, A. A.; Zhang, K.; Nolan, S. P.; de la Vega, R. L.; Mukerjee, S. L.; Hoff, C. D.; Kubas, G. J. *Organometallics* **1988**, *7*, 2429–2435.
(48) Muckerman, J. T.; Fujita, E.; Hoff, C. D.; Kubas, G. J. *J. Phys. Chem. B* **2007**, *111*, 6815–6821.
(49) Burk, M. J.; Segmuller, B.; Crabtree, R. H. *Organometallics* **1987**, *6*, 2241–2246.
(50) Conroy-Lewis, F. M.; Redhouse, A. D.; Simpson, S. J. *J. Organomet. Chem.* **1989**, *366*, 357–367.
(51) Bush, M. A.; Hardy, A. D. U.; Manojlovic-Muir, L.; Sim, G. A. *J. Chem. Soc. (A)* **1971**, 1003–1009.
(52) Horton, A. D.; Mays, M. J.; Adatia, T.; Henrick, K.; McPartlin, M. *J. Chem. Soc., Dalton Trans.* **1988**, 1683–1688.
(53) Kulawiec, R. J.; Crabtree, R. H. *Coord. Chem. Rev.* **1990**, *99*, 89–115.
(54) (a) Beck, W.; Schloter, K. *Z. Naturforsch.* **1978**, *33b*, 1214–1222. (b) Fernández, J. M.; Gladysz, J. A. *Organometallics* **1989**, *8*, 207–219. (c) Peng, T.-S.; Winter, C. H.; Gladysz, J. A. *Inorg. Chem.* **1994**, *33*, 2534–2542.
(55) (a) Newbound, T. D.; Colsman, M. R.; Miller, M. M.; Wulfsberg, G. P.; Anderson, O. P.; Strauss, S. H. *J. Am. Chem. Soc.* **1989**, *111*, 3762–3764. (b) Colsman, M. R.; Newbound, T. D.; Marshall, L. J.; Noirot, M. D.; Miller, M. M.; Wulfsberg, G. P.; Frye, J. S.; Anderson, O. P.; Strauss, S. H. *J. Am. Chem. Soc.* **1990**, *112*, 2349–2362. (c) Bown, M.; Waters, J. M. *J. Am. Chem. Soc.* **1990**, *112*, 2442–2443. (d) Arndtsen, B. A.; Bergman, R. G. *Science* **1995**, *270*, 1970–1973. (e) Butts, M. D.; Scott, B. L.; Kubas, G. J. *J. Am. Chem. Soc.* **1996**, *118*, 11831–11843. (f) Huang, D.; Huffman, J. C.; Bollinger, J. C.; Eisenstein, O.; Caulton, K. G. *J. Am. Chem. Soc.* **1997**, *119*, 7398–7399. (g) Huang, D.; Bollinger, J. C.; Streib, W. E.; Folting, K.; Young, V., Jr.; Eisenstein, O.; Caulton, K. G. *Organometallics* **2000**, *19*, 2281–2290. (h) Fang, X.; Huhmann-Vincent, J.; Scott, B. L.; Kubas, G. J. *J. Organomet. Chem.* **2000**, *609*, 95–103. (i) Tellers, D. M.; Bergman, R. G. *J. Am. Chem. Soc.* **2001**, *123*, 11508–11509. (j) Wu, F.; Dash, A. K.; Jordan, R. F. *J. Am. Chem. Soc.* **2004**, *126*, 15360–15361. (k) Zhang, J.; Barakat, K. A.; Cundari, T. R.; Gunnoe, T. B.; Boyle, P. D.; Petersen, J. L.; Day, C. S. *Inorg. Chem.* **2005**, *44*, 8379–8390.
(56) Hughes, R. P.; Lindner, D. C.; Smith, J. M.; Zhang, D.; Incarvito, C. D.; Lam, K.-C.; Liable-Sands, L. M.; Sommer, R. D.; Rheingold, A. L. *J. Chem. Soc., Dalton Trans.* **2001**, 2270–2278.
(57) Koelle, U. *Coord. Chem. Rev.* **1994**, *135/136*, 623–650.
(58) Kubas, G. J.; Burns, C. J.; Khalsa, G. R. K.; Van Der Sluys, L. S.; Kiss, G.; Hoff, C. D. *Organometallics* **1992**, *11*, 3390–3404.

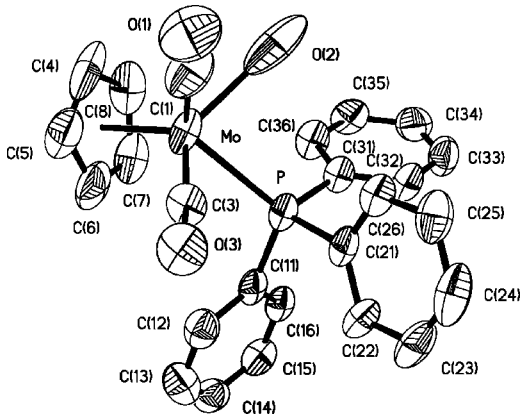

Figure 10. ORTEP diagram (30% probability ellipsoids) of $[Cp(CO)_2(PPh_3)Mo(OH_2)]^+$ (hydrogen atoms not shown).

Table 7. Selected Bond Distances (Å) and Angles (deg) for $[Cp(CO)_2(PPh_3)Mo(OH_2)]^+$

Bond Distances		Bond Angles	
Mo−C(1)	1.955(8)	C(1)−Mo−C(3)	74.7(4)
Mo−C(3)	1.958(11)	C(1)−Mo−O(2)	77.3(3)
Mo−P	2.526(2)	C(3)−Mo−O(2)	126.9(2)
Mo−O(2)	2.445(9)	C(1)−Mo−P	120.8(2)
		C(3)−Mo−P	76.5(2)
		O(2)−Mo−P	80.68(12)

Intentional addition of water to a solution of $[Cp(CO)_2(\eta^3\text{-}PPh_3)Mo]^+[BAr'_4]^-$ led to the isolation of $[Cp(CO)_2(PPh_3)Mo(OH_2)]^+[BAr'_4]^-$ as red crystals in 78% yield. The crystal structure was determined at the National Synchrotron Light Source. There is some static disorder in this crystal, as the coordinated water and one of the carbonyl ligands (C(3)−O(3)) are disordered between the two coordination sites. Attempts to refine a model using a water molecule and a carbonyl ligand sharing the same coordination site (in an approximately 75:25 ratio for one site and 25:75 for the other position) did not result in a better model because the atoms sharing the coordination site in the disordered model were only about 0.6 Å apart. This disordering and the choice of including only the predominant ligand in each site is responsible for the elongated thermal ellipsoid of O(2).

An ORTEP diagram is shown in Figure 10, and selected bond distances and angles are listed in Table 7. Hydrogen bonding between water ligands and counterions is almost invariably found with anions such as BF_4^- or OTf^-, but is expected to be less prevalent with counterions such as BAr'_4^-. The closest distance between O(2) and an F on one of the CF_3 groups of the BAr'_4^- anion is 3.17 Å. Much shorter F···O contact distances of 2.804 and 2.805 Å were found between the water ligand and fluorine atoms of the $CF(CF_3)_2$ ligand in the crystal structure of $\{Cp^*(PMe_3)Ir[CF(CF_3)_2]\}^+ \cdot 0.5\ OH_2[BAr'_4]^-$.[56] The structure of $[Cp(CO)_2(PPh_3)Mo(OH_2)]^+[BAr'_4]^-$ has a carbonyl oxygen [O(1)] that is 3.1 Å from O(2), again indicating at most a very weak hydrogen bond. Our interpretation of these data is that hydrogen bonding of the OH_2 ligand to either O or F in the crystal structure of $[Cp(CO)_2(PPh_3)Mo(OH_2)]^+[BAr'_4]^-$ is not present or is, at most, a very weak interaction.

The ^{1}H NMR resonance for H_2O ligands in organometallic complexes is often broad, and its chemical shift is variable and dependent on temperature and concentration. Exchange between free and bound water can cause broadening of the bound water peak, and hydrogen bonding of the bound water ligand can affect its chemical shift. Our ^{1}H NMR spectra of $[Cp(CO)_2(PPh_3)Mo(OH_2)]^+[BAr'_4]^-$ generally showed a broad resonance between δ 2.87 and 3.31 for the H_2O ligand. Many complexes contain both phosphines and water ligands, yet P−H coupling is seldom observed. We were able to determine the P−H coupling between the H on the water ligand and the phosphorus in $[Cp(CO)_2(PPh_3)Mo(OH_2)]^+$. Protonation of $Cp(CO)_2(PPh_3)MoH$ with $[H(Et_2O)_2]^+BAr'_4{}^-$[59] in CD_2Cl_2 produced a mixture of $[Cp(CO)_2(\eta^3\text{-}PPh_3)Mo]^+[BAr'_4]^-$ and $[Cp(CO)_2(PPh_3)Mo(OH_2)]^+[BAr'_4]^-$. The ^{1}H NMR resonance for the OH_2 ligand was observed at δ 3.47 as a doublet ($^3J_{PH}$ = 3.0 Hz). Evolution of H_2 (δ4.59) was observed by NMR and results from decomposition of the cationic dihydride $[Cp(CO)_2(PPh_3)Mo(H)_2]^+$ or the dihydrogen complex $[Cp(CO)_2(PPh_3)Mo(\eta^2\text{-}H_2)]^+$. No intermediate dihydride or dihydrogen complex was observed. The tungsten dihydride $[Cp(CO)_2(PMe_3)W(H)_2]^+OTf^-$ has been characterized by X-ray crystallographically.[60] The related Mo complex might also be a dihydride, but Poli and co-workers studied protonation of $Cp(CO)_2(PMe_3)MoH$ and found prompt evolution of H_2 even at low temperature; they suggested that an unstable dihydrogen complex was formed.[61] Regardless of whether the product of protonation of $Cp(CO)_2(PPh_3)MoH$ is a dihydride or dihydrogen complex, H_2 is produced upon treatment of the metal hydride with acid, and the formation of $[Cp(CO)_2(PPh_3)Mo(OH_2)]^+$ results from adventitious water. Brookhart's acid,[59] $[H(Et_2O)_2]^+BAr'_4{}^-$ is known to be notoriously difficult to obtain completely dry,[62] so it is not so surprising that the aqua complex is formed.

When the solvent is pumped off of solutions containing $[Cp(CO)_2(PPh_3)Mo(OH_2)]^+$, the water ligand is lost, and most of the product is converted to $[Cp(CO)_2(\eta^3\text{-}PPh_3)Mo]^+$. We were unable to reliably determine the K_{eq} of this reaction, but qualitatively it appears to be roughly similar to that observed in eq 3. The observation of water as a ligand in this type of Mo complex is relevant since we have shown that $[Cp(CO)_2(\eta^3\text{-}PPh_3)Mo]^+[BAr'_4]^-$ serves as a catalyst precursor for ionic hydrogenation[63] of ketones.[17] While the main product of these hydrogenations is the alcohol produced by hydrogenation of the C═O bond of the ketone, we also find that small amounts of the alcohol condense to form ethers. This condensation also produces water; so if strong irreversible binding of the water were to occur, then the catalytic activity would be impeded. Facile displacement of water is therefore important in our catalytic reactions.

Conclusion

PPh_3 exhibits a remarkable versatility of bonding modes as a ligand in organometallic complexes. While it most often functions as a traditional two-electron donor, it is also capable of bonding as a chelating ligand in the η^3-PPh_3 mode with a C═C bond to the metal or through interaction of the metal with an agostic C−H bond. Spectroscopic, structural, and computational studies on $[Cp(CO)_2(\eta^3\text{-}PPh_3)Mo]^+$ show bonding of the Mo to a C═C of the Ph ring. Caulton has found examples of Ir complexes where the influence of steric bulk favors agostic interactions, in which bulky ligands push a C−H bond close enough to the metal to engage in an agostic bond.[35] In contrast,

(59) Brookhart, M.; Grant, B.; Volpe, A. F., Jr. *Organometallics* **1992**, *11*, 3920–3922.
(60) Bullock, R. M.; Song, J.-S.; Szalda, D. J. *Organometallics* **1996**, *15*, 2504–2516.
(61) Quadrelli, E. A.; Kraatz, H.-B.; Poli, R. *Inorg. Chem.* **1996**, *35*, 5154–5162.
(62) (a) Hughes, R. P.; Lindner, D. C.; Rheingold, A. L.; Yap, G. P. A. *Inorg. Chem.* **1997**, *36*, 1726–1727. (b) Stahl, S. S.; Labinger, J. A.; Bercaw, J. E. *Inorg. Chem.* **1998**, *37*, 2422–2431.
(63) Bullock, R. M. *Chem.−Eur. J.* **2004**, *10*, 2366–2374.

steric pressure is *not required* to facilitate an interaction of $[Cp(CO)_2(PPh_3)Mo]^+$ with the C═C bond; computational studies on $[Cp(CO)_2(PH_2Ph)Mo]^+$ show that this complex (with a less sterically hindered phosphine than PPh_3) also has a bonding interaction of the C═C with the metal. Computations on $[Cp(CO)_2(PH^tBuPh)Mo]^+$ show that it maintains the bond of a C═C to the metal, rather than forming an agostic interaction of the metal to a C−H of the ^{t}Bu group. The requirements for the different modes of bonding for agostic C−H ligands vs C═C result in distinct structural preferences, though both are relatively weak bonding interactions. When a C−H of a phenyl group of a PPh_3 ligand engages in an agostic bond, the metal is generally located close to the plane of the arene ring. In contrast, in the interaction of the metal with the C═C fragment of an arene ring, the dihedral angle between the plane of the aromatic ring and the plane containing the metal and the two interacting C═C carbons is about 60°. Our results show that bonding of a metal to the C═C bond of an arene can be significantly favored over the more commonly observed agostic C−H bonding.

Experimental Section

General Procedures. All manipulations were carried out under an atmosphere of argon using Schlenk or vacuum-line techniques, or in a Vacuum Atmospheres drybox. ^{1}H NMR chemical shifts were referenced to the residual proton peak of CD_2Cl_2 at δ 5.32. Elemental analyses were carried out by Schwarzkopf Microanalytical Laboratory (Woodside, NY). NMR spectra were recorded on a Bruker AM-300 spectrometer (300 MHz for ^{1}H). IR spectra were recorded on a Mattson Polaris FT-IR spectrometer. $Cp(CO)_2(PPh_3)MoH$,[64] $Ph_3C^+BAr'_4{}^-$[65] [Ar′ = 3,5-bis(trifluoromethyl)phenyl], and $[H(Et_2O)_2]^+BAr'_4{}^-$[59] were prepared by literature methods. $Ph_3C^+BF_4^-$ was purchased from Aldrich and purified by recrystallization from CH_2Cl_2/Et_2O. THF, Et_2O, and hexane were distilled from Na/benzophenone, and CH_2Cl_2 was distilled from P_2O_5.

Preparation of $[Cp(CO)_2(PPh_3)Mo]^+[BAr'_4]$. A solution of $Cp(CO)_2(PPh_3)MoH$ (300 mg, 0.625 mmol) in CH_2Cl_2 (12 mL) was added to a cold (−30 °C) solution of $Ph_3C^+BAr'_4{}^-$ (665 mg, 0.600 mmol) in CH_2Cl_2 (10 mL). The reaction mixture turned dark red and was stirred at −30 °C for 20 min. The solvent was reduced to 5 mL, and purple solids precipitated. Hexane (20 mL) was added, and the precipitate was collected by filtration, washed with hexane (3 × 10 mL), and dried under vacuum to give $[Cp(CO)_2(PPh_3)Mo]^+[BAr'_4]^-$ (700 mg, 84%) as a tan solid. ^{1}H NMR (CD_2Cl_2, 22 °C): δ 7.80−7.20 (br m, 27 H, B*Ar′*$_4$ + P*Ph*$_3$), 5.62 (s, 5 H, *Cp*). ^{31}P{^{1}H} NMR (CD_2Cl_2, 295 K): δ 38.3 (s). IR (CH_2Cl_2): ν(CO) 2009 (s), 1939 (s) cm^{-1}. IR (Nujol): ν(CO) 2019 (s), 1956 (s) cm^{-1}. Anal. Calcd for $C_{57}H_{32}BF_{24}O_2PMo$: C, 50.99; H, 2.40. Found: C, 50.45; H, 2.24. This complex decomposes to unidentified products over several days at room temperature in CD_2Cl_2 solution. ^{1}H NMR (CD_2Cl_2, −60 °C): the signals for $BAr'_4{}^-$ (δ 7.74 and 7.53) overlapped with the signals of PPh_3 (δ 7.82−7.20), δ 6.12 (br t, 1 H, C*H*, $^3J_{HH} \sim {}^3J_{PH}$ = 6.9 Hz) (with ^{1}H decoupling at the aromatic protons δ 7.37, the triplet at δ 6.12 collapsed to a doublet with J_{PH} = 7.7 Hz), 5.62 (s, 5 H, *Cp*). ^{13}C{^{1}H} NMR (CD_2Cl_2, −60 °C): δ 237.0 (d, J_{CP} = 24.8, *C*O), 231.4 (s, *C*O), 161.4 (1:1:1:1 quartet, J_{CB} = 50.9 Hz, *ipso*-C of $BAr'_4{}^-$), 135.2 (s, *p*-C of P*Ph*Ph$_2$), 134.3 (br s, *o*-C of $BAr'_4{}^-$), 134.0 (d, J_{CP} = 11.6 Hz, *o*-C of PPh*Ph*$_2$), 134.0 (s, *p*-C of PPh*Ph*$_2$), 133.6 (d, J_{CP} = 12.1 Hz, *o*-C of PPh*Ph*$_2$), 133.1 (d, J_{CP} = 13.7 Hz, *m*-C of P*Ph*Ph$_2$), 132.2 (d, J_{CP} = 10.9 Hz, *o*-C′ of P*Ph*Ph$_2$), 129.9 (d, J_{CP} = 11.8 Hz, *m*-C of PPh*Ph*$_2$), 129.6 (d, J_{CP} = 12.4 Hz, *m*-C of PPh*Ph*$_2$), 128.3 (br, q, J_{CF} = 31 Hz, *m*-C of $BAr'_4{}^-$), 126.2 (d, J_{CP} = 53.0 Hz, *ipso*-C of PPh*Ph*$_2$), 124.1 (q, J_{CF} = 272 Hz, *C*F$_3$ of $BAr'_4{}^-$), 121.7 (d, J_{CP} = 60 Hz, *ipso*-C of PPh*Ph*$_2$), 117.2 (br s, *p*-C of $BAr'_4{}^-$), 94.4 (s, *Cp*), 90.0 (d, J_{CP} = 11.8 Hz, *o*-C of P*Ph*Ph$_2$), 81.5 (d, J_{CP} = 28.6 Hz, *ipso*-C of P*Ph*Ph$_2$). ^{31}P{^{1}H} NMR (CD_2Cl_2, −60 °C): δ 37.6 (s).

Crystal Formation of $[Cp(CO)_2(PPh_3)Mo]^+[BAr'_4]^-$. In a glovebox, ~70 mg of $[Cp(CO)_2(PPh_3)Mo]^+[BAr'_4]^-$ was dissolved in toluene (~15 mL) to make a saturated solution. The mixture was filtered into a Schlenk tube and cooled to 0 °C. After 20 days, red crystals were collected and dried by blowing Ar over them. One toluene molecule was found in the crystal structure.

Synthesis and Crystal Growth of $[Cp(CO)_2(PPh_3)Mo(ICH_3)]^+[BAr'_4]^-$. In a glovebox, $[Cp(CO)_2(PPh_3)Mo]^+[BAr'_4]^-$ (45 mg; 0.033 mmol) was dissolved in toluene (5 mL) and CH_2Cl_2 (1.5 mL). Then CH_3I (15 μL, 0.24 mmol, 7.3 equiv) was added, and the solution was filtered into a Schlenk tube. Hexane (~7 mL) was layered on top, and the solution was cooled in a freezer (−20 °C) for 6 days. The red crystals (32 mg, 64% yield) were collected by filtration and dried by blowing Ar over them (not dried under vacuum). Anal. Calcd for $C_{58}H_{35}BF_{24}IO_2PMo$: C, 46.93; H, 2.38. Found: C, 47.31; H, 2.30. ^{1}H NMR (CD_2Cl_2, 22 °C): δ 7.72 (br, 8 H, *o*-H of $BAr'_4{}^-$), 7.73−7.50 (br m, 13 H, *p*-H of $BAr'_4{}^-$ + P*Ph*$_3$), 7.28−7.22 (m, 6 H, P*Ph*$_3$), 5.55 (s, 5 H, *Cp*), 2.38 (s, 3 H, C*H*$_3$). ^{31}P{^{1}H} NMR (22 °C): δ 46.5 (s). ^{13}C NMR (−60 °C): 241.7 (d, J_{CP} = 29.0 Hz, *C*O), 240.9 (s, *C*O), 161.4 (1:1:1:1 quartet, J_{CB} = 49.7 Hz, *ipso*-C of $BAr'_4{}^-$), 134.2 (s, *o*-C of $BAr'_4{}^-$), 133.0−129.1 (m, PPh_3), 128.2 (br q, J_{CF} = 30.1 Hz, *m*-C of $BAr'_4{}^-$), 124.0 (q, J_{CF} = 272.4 Hz, *C*F$_3$ of $BAr'_4{}^-$), 117.2 (s, *p*-C of $BAr'_4{}^-$), 94.6 (s, *Cp*), −6.0 (d, $^3J_{CP}$ = 4.5 Hz, IC*H*$_3$). IR (CH_2Cl_2): ν(CO) 1987 (s), 1917 (s) cm^{-1}. IR (Nujol): ν(CO) 1992 (s), 1927 (s) cm^{-1}. (Spectra of free CH_3I in CD_2Cl_2 for comparison: ^{1}H NMR (22 °C) δ 2.16 (s); ^{13}C{^{1}H} NMR (−60 °C) δ −21.2 (s).)

When a solution of $[cis\text{-}Cp(CO)_2(PPh_3)Mo(ICH_3)]^+$ was pumped to dryness and redissolved in CD_2Cl_2, the ^{1}H NMR showed that 71% of $cis\text{-}Cp(CO)_2(PPh_3)Mo(ICH_3)^+$ remained, but $trans\text{-}Cp(CO)_2(PPh_3)Mo(ICH_3)^+$ (4%) and $[Cp(CO)_2(PPh_3)Mo]^+[BAr'_4]^-$ (25%) were formed. Partial ^{1}H NMR for $[trans\text{-}Cp(CO)_2(PPh_3)Mo(ICH_3)]^+$: δ 5.33 (d, *Cp*, J_{PH} = 1.9 Hz), 2.60 (s, C*H*$_3$). ^{31}P{^{1}H} NMR of $[trans\text{-}Cp(CO)_2(PPh_3)Mo(ICH_3)]^+[BAr'_4]^-$: δ 54.1 (s). After 22 h, the NMR spectrum showed a mixture of $[cis\text{-}Cp(CO)_2(PPh_3)Mo(ICH_3)]^+$ (45%), $[trans\text{-}Cp(CO)_2(PPh_3)Mo(ICH_3)]^+$ (30%), $[Cp(CO)_2(PPh_3)Mo]^+[BAr'_4]^-$ (18%), and unidentified decomposition products (7%).

Determination of the K_{eq} for Formation of $[Cp(CO)_2(PPh_3)Mo(ICH_3)]^+[BAr'_4]^-$. $[Cp(CO)_2(PPh_3)Mo]^+[BAr'_4]^-$ (30.0 mg, 0.0223 mmol) was placed in a NMR tube along with CD_2Cl_2 and 1,2-dichloroethane (0.6 μL, internal standard) to give a total volume of 0.53 mL, with the concentration of $[Cp(CO)_2(PPh_3)Mo]^+[BAr'_4]^-$ = 42 mM. After the initial spectra were taken, CH_3I (2.5 μL, 0.040 mmol, 1.80 equiv) was added. ^{1}H and ^{31}P NMR spectra recorded at 22 °C indicated equilibrium concentrations of 40 mM $[cis\text{-}Cp(CO)_2(PPh_3)Mo(ICH_3)]^+[BAr'_4]^-$, 2.3 mM $[Cp(CO)_2(PPh_3)Mo]^+[BAr'_4]^-$, and 34 mM free ICH_3; K_{eq} = 5.2 × 10^2 M^{-1}.

Synthesis and Crystal Growth of $[Cp(CO)_2(PPh_3)Mo(OH_2)]^+[BAr'_4]^-$. In a glovebox, $[Cp(CO)_2(PPh_3)Mo]^+[BAr'_4]^-$ (50 mg, 0.037 mmol) was dissolved in toluene (5 mL) and CH_2Cl_2 (2.5 mL). The solution was filtered into a Schlenk tube, which was removed from the glovebox. H_2O (1.5 μL, 0.083 mmol, 2.3 equiv) was added, and the solution was layered with hexane (3 mL) cooled at −20 °C for 7 days. Red crystals (40 mg, 0.029 mmol, 78% yield) were collected by filtration and dried by blowing Ar over them (not dried under vacuum). Anal. Calcd for $C_{57}H_{34}BF_{24}O_3PMo$: C, 50.32; H, 2.52. Found: C, 50.36; H, 2.50. NMR (CD_2Cl_2, 22 °C): δ 7.72 (br, 8 H, *o*-H), 7.73−7.50 (br m, 13 H, *p*-H of $BAr'_4{}^-$ + P*Ph*$_3$), 7.28−7.22 (m, 6 H, P*Ph*$_3$), 5.58 (s, 5 H, *Cp*). In isolated

(64) Bainbridge, A.; Craig, P. J.; Green, M. *J. Chem. Soc. (A)* **1968**, 2715–2718.
(65) Bahr, S. R.; Boudjouk, P. *J. Org. Chem.* **1992**, *57*, 5545–5547.

Table 8. Crystallographic Data Collection and Refinement Information

	$[Cp(CO)_2(PPh_3)Mo]^+[BAr'_4]^-$	$[Cp(CO)_2(PPh_3)Mo\text{-}(OH_2)]^+[BAr'_4]^-$	$[Cp(CO)_2(PPh_3)Mo\text{-}(ICH_3)]^+[BAr'_4]^-$
formula	$C_{64}H_{40}BMoF_{24}O_2P$	$C_{64}H_{42}BMoF_{24}O_3P$	$C_{58}H_{35}BMoF_{24}O_2IP$
fw	1434.68	1452.70	1484.48
temp (K)	95(2)	95(2)	293(2)
cryst syst	monoclinic	triclinic	triclinic
space group	$P2_1/n$ (No. 14)	$P\bar{1}$ (No. 2)	$P\bar{1}$ (No. 2)
a (Å)	15.371(2)	13.792(4)	12.421(2)
b (Å)	24.095(2)	15.032(6)	13.151(2)
c (Å)	17.319(2)	16.414(7)	18.319(5)
α (deg)		69.08(2)	96.53(2)
β (deg)	106.67(2)	72.550(10)	96.34(2)
γ (deg)		82.62(2)	90.11(2)
V (Å^3)	6144.8(12)	3032(2)	2954.5(10)
Z	4	2	2
μ (mm^{-1})	12.2	9.53	0.889
λ (Å)	1.100	1.008	0.71073
ρ_{calc} (g cm^{-3})	1.551	1.591	1.669
cryst size (mm)	0.08 × 0.08 × 0.02	0.33 × 0.27 × 0.03	0.52 × 0.30 × 0.11
2θ range (deg)	2.31 to 37.00	3.67 to 38.43	1.13 to 24.99
total no. of reflns	18 041	17 076	10 322
no. of indep reflns, $I \geq 3.0\sigma(I)$	5504 [R(int) = 0.076]	6736 [R(int) = 0.061]	10 322
no. of params	674	851	795
final R indices [$I > 2\sigma(I)$][a]	R1 = 0.0738, wR2 = 0.1899	R1 = 0.0689, wR2 = 0.2088	R1 = 0.0609, wR2 = 0.1377
R indices (all data)	R1 = 0.0981, wR2 = 0.2097	R1 = 0.0863, wR2 = 0.2409	R1 = 0.2345, wR2 = 0.1981
goodness-of-fit on $F2$	1.016	1.112	0.999
extinction coeff	none	0.0064(9)	none
absorp corr	Fourier(XABS2)[b]	none	Gaussian

[a] $R1 = \sum||F_o| - |F_c||/\sum|F_o|$; $wR2 = \{\sum[w(|F_o^2| - |F_c^2|)^2]/\sum[w|F_o^2|^2]\}^{1/2}$. [b] Parkin, S.; Moezzi, B.; Hope, H. *J. Appl. Crystallogr.* **1995**, *28*, 53−56.

samples and NMR tube preparations, the position of the resonance of the OH_2 ligand varied between δ 2.87 and 3.31 (br, 2 H, OH_2). It was usually broad (except as described for one case below), but the integration (2H) confirms its assignment. $^{31}P\{^1H\}$ NMR of [*cis*-$Cp(CO)_2(PPh_3)Mo(OH_2)]^+BAr'_4{}^-$: δ 55.1 (s). ^{13}C NMR (CD_2Cl_2, 233 K): 250.5 (d, J_{CP} = 29.4 Hz, *C*O), 248.2 (s, *C*O), 161.6 (1:1:1:1 quartet, J_{CB} = 49.6 Hz, *ipso*-C of $BAr'_4{}^-$), 134.5 (*o*-C of $BAr'_4{}^-$), 133.0 (d, J_{C-P} = 11.2 Hz, *o*-C of PPh_3), 132.1 (s, *p*-C of PPh_3), 131.2 (br d, J_{CP} = 54.3 Hz, *ipso*-C of PPh_3), 129.8 (d, J_{CP} = 10.3 Hz, *m*-C of PPh_3), 128.5 (br q, J_{CF} = 32.5 Hz, *m*-C of $BAr'_4{}^-$), 124.3 (q, J_{CF} = 272.5 Hz, *C*F_3 of $BAr'_4{}^-$), 117.4 (*p*-C of $BAr'_4{}^-$), 96.1 (s, *Cp*). IR (CH_2Cl_2): ν(CO) 1985 (s), 1909 (s) cm^{-1}. IR (Nujol): ν(CO) 1984 (s), 1887 (s) cm^{-1}.

NMR Tube Reaction of $Cp(CO)_2(PPh_3)MoH$ with $H(Et_2O)_2$-$BAr'_4{}^-$ in CD_2Cl_2. A 5 mm NMR tube equipped with a Teflon J. Young valve was charged with $Cp(CO)_2(PPh_3)MoH$ (7.7 mg, 0.016 mmol) and $H(Et_2O)_2BAr'_4{}^-$ (19.6 mg, 0.019 mmol). CD_2Cl_2 (∼0.5 mL) was added into this tube to give a red solution. The formation of H_2 (δ 4.59) was observed. The NMR spectra indicated the formation of $[Cp(CO)_2(PPh_3)Mo(OH_2)]^+[BAr'_4]^-$ (65%) and $[Cp(CO)_2(PPh_3)Mo]^+[BAr'_4]^-$ (35%). ^1H NMR for $[Cp(CO)_2(PPh_3)$-$Mo(OH_2)]^+[BAr'_4]^-$ were as described above, with the notable exception of the H_2O ligand, which appeared at δ 3.47 (d, 2 H, $^3J_{PH}$ = 3.0 Hz, H_2O). The solvent was removed under vacuum, and the residue was redissolved in CD_2Cl_2. The NMR spectra showed that most (89%) of the product was $[Cp(CO)_2$-$(PPh_3)Mo]^+[BAr'_4]^-$, with 11% of $[Cp(CO)_2(PPh_3)Mo(OH_2)]^+$-$[BAr'_4]^-$ remaining.

Determination and Refinement of the Crystal Structures. Attempts to determine the structures of $[Cp(CO)_2(PPh_3)$-$Mo]^+[BAr'_4]^-$ and $[Cp(CO)_2(PPh_3)Mo(OH_2)]^+[BAr'_4]^-$ with a conventional X-ray source (sealed tube) were not successful, since the crystals were small and poor diffractors of X-rays. These crystals were coated with perfluoropolyether oil and mounted on the end of a glass capillary; data were collected at 95 K using X-rays from the National Synchrotron Light Source at Brookhaven National Laboratory. For $[Cp(CO)_2(PPh_3)Mo(ICH_3)]^+[BAr'_4]^-$ crystals were coated with Vaseline and sealed inside a glass capillary, which was transferred to an Enraf Nonius CAD-4 diffractometer. Diffraction data indicated monoclinic symmetry and systematic absences consistent with space group $P2_1/n$ for $[Cp(CO)_2(PPh_3)$-$Mo]^+[BAr'_4]^-$; triclinic symmetry for $[Cp(CO)_2(PPh_3)Mo(OH_2)]^+$-$[BAr'_4]^-$ and $[Cp(CO)_2(PPh_3)Mo(ICH_3)]^+[BAr'_4]^-$ consistent with the space groups $P1$ and $P\bar{1}$. In the least-squares refinement, anisotropic temperature parameters were used for all the non-hydrogen atoms in $[Cp(CO)_2(PPh_3)Mo(OH_2)]^+[BAr'_4]^-$ and $[Cp(CO)_2(PPh_3)Mo(ICH_3)]^+[BAr'_4]^-$. For $[Cp(CO)_2(PPh_3)Mo]^+$-$[BAr'_4]^-$, anisotropic temperature parameters were used for all the non-hydrogen atoms except the boron and carbons in the anion. Hydrogen atoms (except those on the toluene of crystallization for $[Cp(CO)_2(PPh_3)Mo]^+[BAr'_4]^-$, which were not included) were placed at calculated positions and allowed to "ride" on the atom to which they were attached.

Acknowledgment. Research at Brookhaven National Laboratory was carried out under contract DE-AC02-98CH10886 with the U.S. Department of Energy and was supported by its Division of Chemical Sciences, Office of Basic Energy Sciences. Research at Pacific Northwest National Laboratory was funded by the Division of Chemical Sciences, Office of Basic Energy Sciences, U.S. Department of Energy, and by an LDRD grant. Pacific Northwest National Laboratory is operated by Battelle for the U.S. Department of Energy.

Supporting Information Available: Coordinates of optimized $[Cp(CO)_2(\eta^3\text{-}PPh_3)Mo]^+$, $[Cp(CO)_2(PH^tBuPh)Mo]^+$, $[Cp(CO)_2(PH_2Ph)$-$Mo]^+$, and $[Cp(CO)_2(PH_2Ph)Nb]$ and crystallographic information (cif files) for $[Cp(CO)_2(\eta^3\text{-}PPh_3)Mo]^+[BAr'_4]^-$, $[Cp(CO)_2(PPh_3)Mo$-$(ICH_3)]^+[BAr'_4]^-$, and $[Cp(CO)_2(PPh_3)Mo(OH_2)]^+[BAr'_4]^-$. This material is available free of charge via the Internet at http://pubs.acs.org.

OM800401D